ACS APPLIED MATERIALS & INTERFACES

Research Article

www.acsami.org

Role of Gold Nanoparticles Capping Density on Stability and Surface Reactivity to Design Drug Delivery Platforms

Juliana Tournebize,[†] Ariane Boudier,[†] Anne Sapin-Minet,[†] Philippe Maincent,[†] Pierre Leroy,[†] and Raphaël Schneider*[,‡]

[†]CITHEFOR EA 3452, Cibles thérapeutiques, formulation et expertise préclinique du médicament, Faculty of Pharmacy, Université de Lorraine, BP 80403, 54001 Nancy Cedex, France

[‡]Laboratoire Réactions et Génie des Procédés, Université de Lorraine, UPR 3349, CNRS, 1, rue Grandville, BP 20451, 54001 Nancy Cedex, France

ABSTRACT: Five-nanometer sized gold nanoparticles (Au NPs) stabilized with citrate ions have been reacted with various amounts of dihydrolipoic acid (DHLA) (×28, ×56, ×140, ×222, relative to Au NPs). Ligand exchange between citrate and the dithiol resulted in DHLA-capped Au NPs, whose degree of inertia was found to be related to the density of capping. The results revealed the importance of DHLA coating density to enhance the colloidal stability and modulate the reactivity toward free radicals and proteins of biological relevance. Thus, Au NPs capped with the highest amount of DHLA were found to be the ones that were, first, the most resistant to environmental changes, then characterized by the lowest residual catalytic reactivity of their metallic core, and finally the lowest interacting with proteins through nonspecific adsorption. The physicochemical properties conferred to Au NPs prepared with the ×222 excess should be valuable for further pharmaceutical development of nanoparticle platforms.

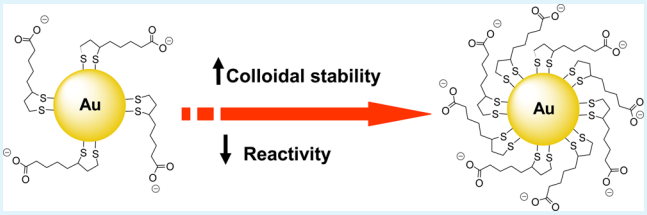

KEYWORDS: *gold nanoparticles, dihydrolipoic acid, capping density, stability, catalytic activity*

1. INTRODUCTION

Functionalized noble-metal nanoparticles (NPs), which specifically interact with cellular targets, are of great interest in biotechnology and medicine.[1−3] Among these metal NPs, and because of their inertia as well as weakly toxic nature, controllable size, and ease of functionalization with various ligands, gold NPs (Au NPs) have been intensively studied recently for diagnostic applications,[4,5] including tomography and magnetic resonance imaging,[6] as well as for drug delivery.[7−9] However, the essential parameters affecting the successful use of Au NPs for biological purposes are their stability in physiological conditions, as well as their surface reactivity toward molecules encountered in living organisms.[10]

The stability of Au NPs dispersions is strongly dependent on their surface charge as well as pH and ionic strength of the medium. Because of these concerns, extensive research is focusing on the improvement of the Au NPs stability and the development of methods to evaluate the stability of Au NPs prior to their biological use. The most common strategy to disperse Au NPs in an aqueous medium and to gain access to NPs valuable for bioapplications is the use of a protective agent, which not only prevents the aggregation of NPs, but also leads to functionalized objects.[11] So far, thiol-containing compounds have been widely used as protective agents for obtaining stable monolayer-protected Au NPs, because of the strong affinity of sulfur to gold.[12] In many cases, the Au NPs are synthesized using Turkevich's method[13] or modifications of this method[14,15] and functionalized via a two-step approach, referred to as "cap exchange" (or ligand exchange). This involves replacing the native citrate cap with bifunctional hydrophilic ligands that contain a thiol group for anchoring the ligand to the nanocrystal surface and a second module that not only promotes aqueous dispersibility[16,17] but also can ease the grafting of a drug via carboxylic acid groups, for example.[18] Regardless of the cap-exchange method used, small hydrodynamic diameters (<25 nm) and good colloidal stability are prerequisite for developing Au NPs with great potential utility in biological applications. The success of these applications largely depends on the ligand used to cap the nanocrystal surface.

Indeed, depending on the targeted application, the ligand type and the density of capping should differ. Thus, as far as catalysis domain is concerned, it was previously shown that, whatever the selected ligand, the capping limits the catalytic activity of Au NPs. Moreover, increasing the capping density was related to a decrease of the catalytic efficiency.[19] In contrast, for biological purposes, a total inertia is required to ensure biocompatibility; therefore, an absence of any residual catalytic activity parallel to an optimized capping density is needed.

Among the various ligand used, dihydrolipoic acid (DHLA, **2**), the reduced form of α-lipoic acid (LA, **1**) (Figure 1), and

Received: July 10, 2012
Accepted: October 29, 2012
Published: October 29, 2012

 © 2012 American Chemical Society dx.doi.org/10.1021/am3012752 | *ACS Appl. Mater. Interfaces* 2012, 4, 5790−5799

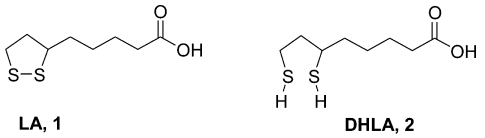

Figure 1. Molecular structures of α-lipoic acid (**1**) and dihydrolipoic acid (**2**).

the poly(ethylene glycol) esters of DHLA are known to afford NPs, such as quantum dots, with higher colloidal stability than monothiol ligands, because of the higher affinity of the dithiol function toward metal atoms present at the nanocrystal surface.[18,20−22]

DHLA, its derivatives, and other multiple thiol-anchor compounds have also been proven to be valuable ligands for stabilizing and inhibiting the aggregation of Au NPs in aqueous solution.[10,23−36] Furthermore, DHLA is a physiological compound, with antioxidant activity, already administered to humans.[37] As a consequence, this molecule has high potential as a Au NP ligand.

Although DHLA-capped Au NPs are a substantial improvement, in term of stability and also biocompatibility,[38] compared to monothiol-stabilized ones, no systematic study devoted to the influence of the [DHLA]/[Au] molar ratio during the cap exchange on the properties of produced Au NPs has been undertaken. In fact, high molar excess of DHLA or its derivatives are generally used to saturate NP surfaces. In this work, cap-exchange reactions of physisorbed bound citrate ions present at the surface of small-sized (ca. 5 nm in diameter) Au NPs prepared via Turkevich's method by using DHLA were investigated. The influence of the molar ratio of DHLA to Au on the aggregation behavior of Au NPs in phosphate buffer solution and in the presence of excess salt was studied. Next, we investigated the role of DHLA capping density on the reactivity with various molecules, a dithiol, a free radical $ABTS^{\bullet+}$, and a protein of biological relevance (albumin). This work highlights how important is the packing density to build a stable and inert platform for the design of drug delivery systems.

2. EXPERIMENTAL SECTION

2.1. Chemicals. All reagents and solvents were of analytic grade and used without further purification. Tetrachloroauric acid trihydrate ($HAuCl_4{\cdot}3H_2O$) and α-lipoic acid were purchased from Sigma−Aldrich (France). Phosphate-buffered saline (PBS) solution was prepared as follows: $[Na_2HPO_4] = 4 \times 10^{-2}$ M, $[KH_2PO_4] = 4 \times 10^{-3}$ M, and $[NaCl] = 1 \times 10^{-1}$ M, final pH was adjusted to 7.4. Ultrapure deionized water (>18.2 MΩ cm) was used to prepare all solutions. All glassware was thoroughly washed using aqua regia (3:1 HCl/HNO_3) and rinsed with ultrapure water prior to use.

2.2. Preparation of Citrate-Stabilized Gold Sols. Gold colloids were prepared at room temperature via the sodium borohydride reduction of $HAuCl_4{\cdot}3H_2O$ in the presence of sodium citrate, as described by Brown and co-workers.[15] Briefly, at room temperature, 1 mL of a 1% (w/v) $HAuCl_4{\cdot}3H_2O$ solution in water was added to 90 mL of water. After 1 min of stirring, 2.0 mL of a 38.8 mM sodium citrate solution in water were added. One minute later, 1.0 mL of a freshly prepared 0.075% (w/v) $NaBH_4$ solution in a 38.8 mM sodium citrate solution was quickly injected in the reaction flask. The reaction medium was stirred for an additional 5-min period and the resulting deep red colloidal solution immediately stored in darkness at 4 °C for a maximum period of 2 months in a polypropylene tube.

2.3. Synthesis and Purification of DHLA-Capped Gold Nanoparticles (Au@DHLA). $Au@DHLA_{28}$, $Au@DHLA_{56}$, $Au@DHLA_{140}$, and $Au@DHLA_{222}$ NPs were prepared by adding, respectively, 90, 150, 375, and 600 μmol of α-lipoic acid, solubilized in, respectively, 1.5, 2.5, 5, and 10 mL of 0.5 M aqueous NaOH solution, to 25 mL of freshly prepared citrate-capped Au NPs. The reaction mixture was stirred for 24 h at a temperature of 20−23 °C before dialysis. The nonreacted α-lipoic acid remaining in the solution after the cap exchange was removed by dialysis against PBS for 48 h using a dialysis bag (regenerated cellulose with a molecular weight cutoff of 10 kDa (Roth, France)). The dialysis medium was changed once to fresh PBS after 24 h. The resulting Au@DHLA NPs suspension was stored in darkness at 4 °C for a maximum period of 2 months in polypropylene tube.

2.4. Characterization of Gold Nanoparticles (Au NPs). A double-beam UV−visible spectrophotometer (model Uvikon 932, Kontron) was used for spectra recordings and absorbance measurements. All measurements were performed at 20−23 °C using quartz cuvettes with a path length of 1 cm. The scanning wavelength range was from 200 nm to 900 nm, with intervals of 0.4 nm. Molar absorbance values of Au NPs were calculated as previously published.[39] The results are the following: $1.20 \pm 0.10 \times 10^7$, $0.43 \pm 0.10 \times 10^7$, $0.43 \pm 0.10 \times 10^7$, $0.42 \pm 0.10 \times 10^7$, and $0.50 \pm 0.20 \times 10^7$ M^{-1} cm^{-1}, for citrate-stabilized Au NPs, $Au@DHLA_{28}$, $Au@DHLA_{56}$, $Au@DHLA_{140}$, and $Au@DHLA_{222}$ NPs, respectively.

Transmission electronic microscopy (TEM) images were recorded using a Philips CM20 instrument with a LaB_6 cathode operating at 200 kV. Au NPs solutions were deposited onto a 400-mesh carbon film copper grids. The average diameter of the gold core was calculated for each Au NP sample by counting ca. 200 individual particles from TEM images. From these observations, the number of Au surface atoms (N_s) on a single Au NP was calculated using the relation

$$N_s = \frac{4\Pi {R_{NP}}^2}{\Pi {R_{atom}}^2}$$

where R_{NP} is the radius obtained by transmission electron microscopy (TEM) and $R_{atom} = 0.137$ nm.[40]

The hydrodynamic diameter (D_h) and surface charge of Au NPs were measured using a Zetasizer Nano ZS (Malvern Instruments, U.K.). These measurements were performed at 20 °C using low-volume polystyrene and disposable capillary cells, respectively. All D_h reported are volume-average values, based on three independent measurements of two Au NPs batches. Prior to zeta potential measurements, Au@DHLA NPs were dialyzed against ultrapure water for 24 h. All surface charges reported are averages based on three measurements at least two batches of Au NPs.

X-ray photoelectron spectroscopy (XPS) measurements were performed at a residual pressure of 10^{-9} mbar, using a Kratos Axis Ultra electron energy analyzer (Kratos Analytical, U.K.) operating with a monochromatic Al Kα source.

2.5. Gold and Sulfur Content. The gold content of the various types of Au NPs was determined using the previously reported methodology.[39] A Varian Model 720-ES inductively coupled plasma−optical emission spectrometry (ICP-OES) device was used for multielemental Au and S analyses.

2.6. Stability Studies. Effects of the [DHLA]/[Au] ratio on the stability of Au NPs were evaluated based on changes in the λ_{max} of the surface plasmon resonance (SPR) band and D_h of Au NPs, which were stored at 4 °C in physiological medium PBS (150 mM) and in polypropylene tubes for 50 days. The Au NPs were wrapped with aluminum foil and stored in darkness throughout the measurement period. The effects of dithiothreitol (DTT) and high concentration of salt on the stability of the various [DHLA]/[Au] ratio were also evaluated. Briefly, DTT and NaCl were added to each preparation of Au NPs to a final concentration of 0.1 and 1 M, respectively. The solution was incubated at 40 °C for 1 min and stored in darkness at room temperature (20−23 °C) in low-volume polystyrene cuvettes for 100 min. For all stability studies, citrate-capped Au NPs were used as control samples.

2.7. Interaction of Gold Nanoparticles with 2,2′-azino-di(3-ethylbenzothiazoline-6-sulfonate) and Bovine Serum Albumin. 2,2′-Azino-di(3-ethylbenzothiazoline-6-sulfonate) ($ABTS^{\bullet+}$ stock solution) was prepared by mixing 5.4 mM ABTS with 1.7 mM

potassium persulfate in PBS and placed in darkness at room temperature for 16 h to give a dark blue solution. Molar concentrations of $ABTS^{\bullet+}$ were calculated using the molar absorbance value previously reported (i.e., $\varepsilon_{734\ nm} = 1.5 \times 10^4\ M^{-1}\ cm^{-1}$).[41] The interaction between $ABTS^{\bullet+}$ and Au NPs was studied as follows: 1125 μL of Au@DHLA NPs and citrate-stabilized Au NPs were reacted with 375 μL of 200 μM $ABTS^{\bullet+}$ solution in PBS. After 2 h of incubation at 20−23 °C, the absorbance of the reaction medium was measured at 734 nm.

Aliquots (500 μL) of a 1.6 μM BSA solution prepared in PBS were mixed with Au NPs in PBS (500 μL); the resulting mixtures were incubated at 37 °C for 1 h. The interaction between BSA and Au NPs was monitored measuring the intrinsic tryptophan fluorescence of BSA (λ_{exc} = 280 nm, λ_{em} = 355 nm)[42] with a spectrofluorimeter (Hitachi F-2000, France). Fluorescence intensities with and without Au NPs (I and I°) were measured and Stern−Volmer equation was used to calculate the related constant:

$$\frac{I^\circ}{I} = 1 + K_{SV}[Q]$$

where K_{SV} is the Stern−Volmer constant and $[Q]$ the concentration of Au NPs, which are the quenchers.[43]

2.8. Statistical Analyses. One-way analysis of variance (SigmaStat 3.1) was used for statistical analyses. For each sample group the equal variance (Levene median) and normality (Kolmogorov−Smirnov) tests were performed.

3. RESULTS AND DISCUSSION

Proof of the Surface Packing Density Variations. Citrate-stabilized Au NPs were first synthesized via the reduction of $HAuCl_4$ using sodium borohydride at room temperature. Using TEM, the average diameter of these NPs was found to be 5.3 ± 1.1 nm (see Figure 2), which is consistent with the synthetic method employed.[15]

The UV−vis absorption spectrum of the citrate-stabilized Au NPs shows a narrow plasmon bandwidth, centered at 517 nm, confirming the small diameter and the weak polydispersity observed by TEM (Figure 2). Using a molar absorbance of $\varepsilon = 1.2 \times 10^7\ M^{-1}\ cm^{-1}$ for these ca. 5-nm-sized Au NPs,[39] the concentration of the citrate-stabilized Au NPs solution was found to be 5.89×10^{16} NPs per liter. An average diameter of 5.3 nm represents ~1147 cubic face-centered structural units in each nanocrystal (using a theoretical lattice parameter of a = 0.408 nm), and 4588 Au atoms per nanocrystal.[44] The number of Au surface atoms on a single Au NPs was estimated to be 1104.

DHLA (**2**) can be covalently bound to the surface of Au NPs either by mixing citrate-capped Au NPs with LA (**1**) at pH 11[45] or by reduction of $HAuCl_4$ with $NaBH_4$ in the presence of **2**.[18] We found that citrate ions could be easily displaced from the surface of Au NPs produced during the first step by incubation for one day with **1** in the crude reaction mixture. During the reaction, the dispersion color changed from pink-red to purple-red. The 5-membered heterocycle of **1** containing the dithiolane ring exhibits a strong absorption at 334 nm. This absorption decreases after treatment with Au NPs. Because dialkyldisulfide adsorption on gold yields unstable complexes,[46] a cleavage of the S−S bond of **1** by $NaBH_4$ remaining in the reaction medium is more likely.[18] When an easily reducible carbonyl derivative such as benzaldehyde was added in the reaction mixture after generation of citrate-capped Au NPs, a rapid reduction of the aldehyde was observed (monitored by using a reversed-phase HPLC system coupled with UV detection), thus confirming the presence of unreacted borohydride after the Au NPs formation step.

Using the two-step synthetic protocol we developed, four samples were prepared with different theoretical [DHLA]/[surface Au atoms] molar ratios (28/1, 56/1, 140/1, and 222/1) to evaluate the influence of the ligand coverage on the properties of Au NPs. These samples are noted $Au@DHLA_{28}$, $Au@DHLA_{56}$, $Au@DHLA_{140}$, and $Au@DHLA_{222}$, respectively. At the end of the DHLA anchorage at the surface of Au NPs, the pH of the reaction mixture was found to be ca. 12, regardless of the Au/LA ratio used. Unbound LA was then removed by dialysis against PBS buffer (pH 7.4). Upon dialysis, the complete disappearance of the dithiolane ring absorption at 334 nm was observed. Figure 3 depicts results obtained for $Au@DHLA_{222}$ NPs.

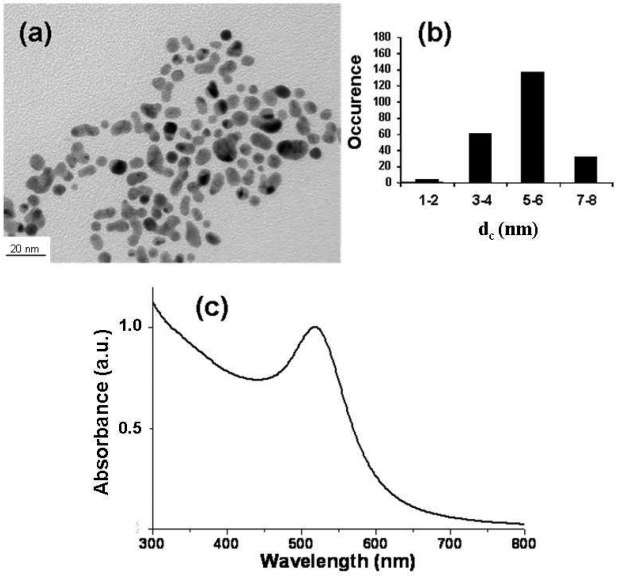

Figure 2. Characteristics of citrate-stabilized Au NPs: (a) TEM image (scale bar = 20 nm), (b) the corresponding size distribution (n > 200), and (c) their UV−vis absorption spectrum.

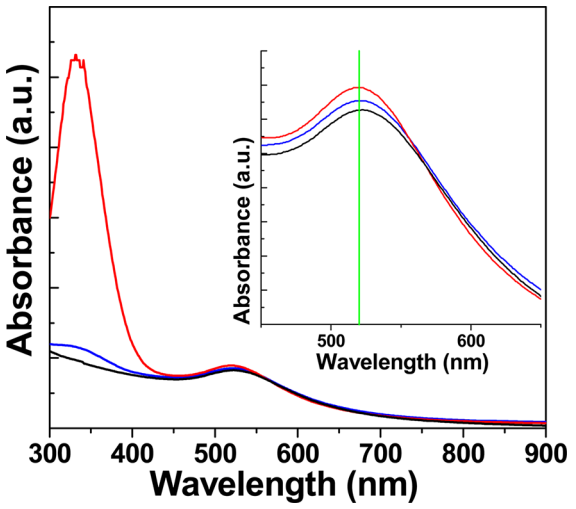

Figure 3. Evolution of the UV−vis spectra of $Au@DHLA_{222}$ NPs, as a function of dialysis time; red, blue, and black traces represent NPs in the reaction medium, NP after 24 h of dialysis, and NPs after 48 h of dialysis, respectively. Inset shows the magnification of the Au NPs surface plasmon resonance band.

dx.doi.org/10.1021/am3012752 | ACS Appl. Mater. Interfaces 2012, 4, 5790−5799

Removal of excess LA was in all cases accompanied by a small bathochromic shift of the SPR band, depending on the NPs ligand coverage. UV−vis absorption spectra showed that, after dialysis, except Au@DHLA$_{28}$ NPs, all NPs exhibit an absorption peak near 520 nm, which is characteristic of the SPR band of Au NPs with an average diameter of 4−5 nm (see Figure 4).

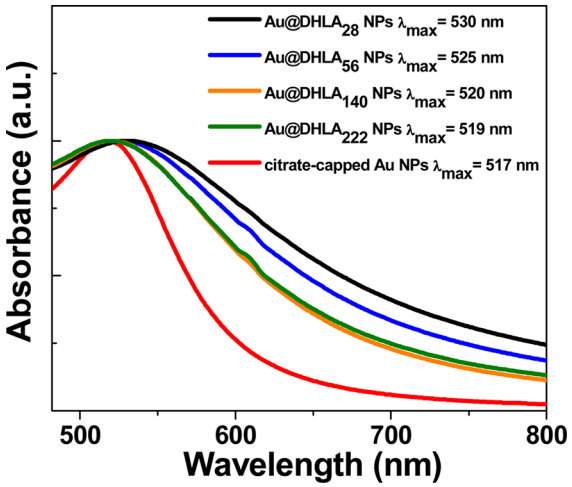

Figure 4. Normalized UV−vis absorption spectra for the several [DHLA]/[Au] molar ratios used during the cap-exchange reaction.

Compared to the SPR band of citrate-stabilized Au NPs (λ_{max} = 517 nm), ligand-exchanged Au@DHLA$_{140}$, and Au@DHLA$_{222}$ NPs exhibit only a slight red shift ($\Delta\lambda$ = 2−3 nm) that may originate either from the NPs surface modification (changes in the surface dielectric constant of the NPs associated with the adsorption of the thiol functions of DHLA) or from the pH decrease of the solution from 12 to 7.4 during dialysis. In complementary experiments performed on dialyzed Au NPs, we observed similar red shifts of the SPR band ($\Delta\lambda$ = 2−3 nm) when decreasing the pH from 12 to 7, probably due to the decrease of interparticle distances, following a decrease of surface charge. However, because these bathochromic shifts were already observed on the crude Au NPs dispersions after the cap exchange before dialysis, we privilege the change of the NPs surface dielectric constant to explain the observed red shifts. These weak red shifts also demonstrate that there is no significant particle aggregation for Au@DHLA$_{140}$ and Au@DHLA$_{222}$ NPs during the cap-exchange process. Some degree of aggregation was observed for Au@DHLA$_{56}$ NPs with a red shift of 8 nm. With the lowest [DHLA]/[Au] ratio used (Au@DHLA$_{28}$ NPs), a more pronounced red shift was observed ($\Delta\lambda$ = 13 nm), indicating a more marked increase of the NPs diameters during the cap exchange. Finally, it can be mentioned that ligands such as thiols, phosphines, or dendrimers can promote core etching of Au NPs during ligand exchange.[47−51] When such ligands are added in limited quantity to Au NPs, only ligand exchange occurs. However, when these ligands are added in excess, an etching of the surface atoms of Au NPs can occur, thus leading to core-size reduction and blue shift of the absorption band. Even if a partial etching may occur during reactions conducted with the highest [DHLA]/[Au] ratios, the close resemblance of the optical spectrum of Au@DHLA NPs with that of the native citrate-capped NPs indicates that etching is a minor synthetic pathway during the citrate → DHLA cap exchange.

X-ray photoelectron spectroscopy (XPS) was first used to confirm the chemical bonding between Au NPs and DHLA. High-resolution spectra collected for Au 4f, S 2p, and C 1s are given in Figure 5. The Au, S, and C signals were compared, and they were found to be similar in shape and position for the four materials prepared by capping exchange. The C 1s peak can be deconvoluted into three peaks associated with C−C bonds (at 284.87 eV), carbon bound to sulfur (at 286.24 eV), and carbon bound to two O atoms (COOH function at 288.16 eV). The presence of these signals corresponds with those expected to be observed after covalent anchorage of DHLA at the surface of Au NPs. The Au 4f region shows a pair of peaks at 83.71 and 87.73 eV assigned to the Au $4f_{7/2}$ and Au $4f_{5/2}$ peaks, respectively, that are originating from the metal gold cores. The peaks of S $2p_{3/2}$ and S $2p_{1/2}$ attributed to S atoms bound to Au NPs are observed at 163.21 and 164.24 eV, respectively, confirming that the S element is linked to the Au surface as thiolate species.[52] Another element detected on the XPS survey scan was oxygen. Gold, carbon, sulfur, and oxygen are consistent with the exclusive structure of the Au@DHLA NPs proposed.

The [S]/[Au] ratio was determined for each Au@DHLA NPs using ICP-OES for S and Au. The results presented in Table 1 showed that the more DHLA was added, the more the Au@DHLA NPs were capped, as expected.

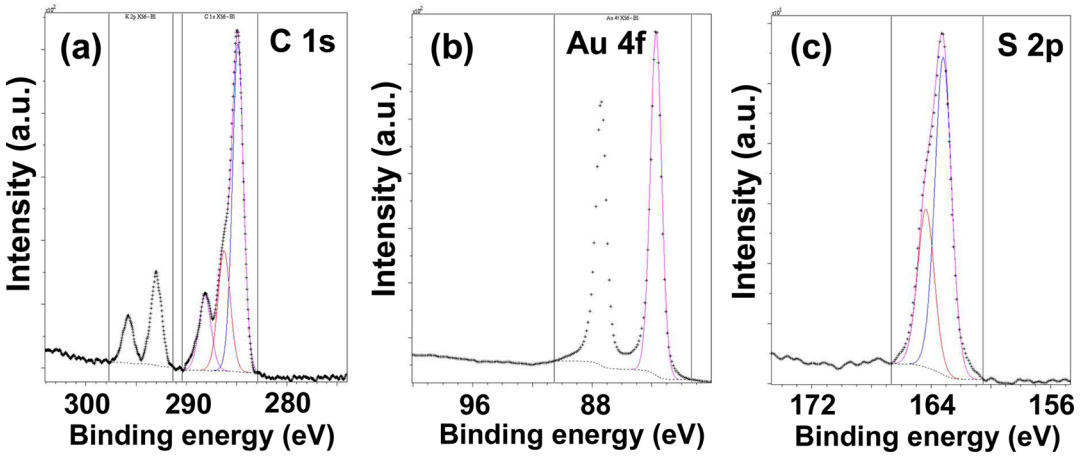

Figure 5. XPS binding energy spectra of Au@DHLA$_{222}$ NPs: (a) C 1s, (b) Au 4f, and (c) S 2p.

Table 1. Characterization of Synthesized Au NPs[a]

	[S]/[Au]	average core diameter, d_c (nm)[b] (n > 200)	hydrodynamic diameter, D_h (nm)[c] (n = 3)	zeta potential, ζ (mV)[d] (n = 3)
citrate-stabilized Au NPs		5.3 ± 1.1	6.5 ± 1.7	−51 ± 2[e]
Au@DHLA$_{28}$	0.26 ± 0.01	6.5 ± 3.5	15.0 ± 1.2	−44 ± 3
Au@DHLA$_{56}$	0.29 ± 0.01	4.0 ± 1.0	7.7 ± 1.2	−56 ± 2
Au@DHLA$_{140}$	0.33 ± 0.02	3.9 ± 1.0	7.7 ± 1.3	−66 ± 5
Au@DHLA$_{222}$	0.41 ± 0.02	3.5 ± 1.3	7.2 ± 1.2	−63 ± 3[e]

[a]Values are expressed as mean ± standard deviation of n independent measurements. [b]As determined by TEM. [c]As determined by DLS. [d]All ζ potential measurements were conducted at pH 7.4. [e]Average ± standard deviation of three batches of Au NPs.

Transmission electron microscopy (TEM), dynamic light scattering (DLS), and zeta potential measurements were further used to determine the physicochemical properties of DHLA-functionalized Au NPs. TEM micrographs (Figure 6) show that spherical shapes dominate in dispersions of Au@DHLA$_{56}$, Au@DHLA$_{140}$, and Au@DHLA$_{222}$ NPs and that these NPs are monodisperse and unaggregated.

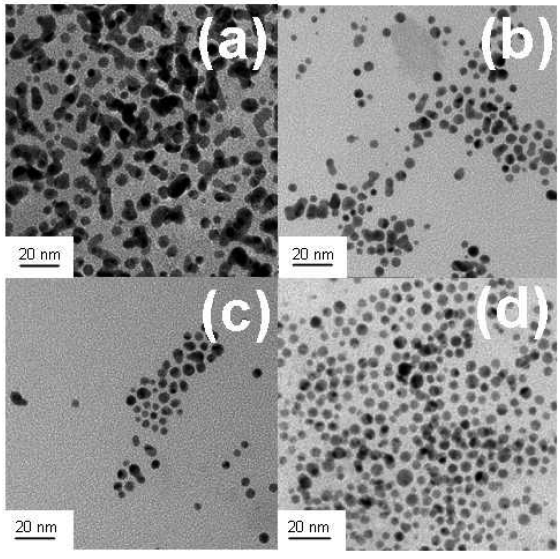

Figure 6. TEM images of (a) Au@DHLA$_{28}$, (b) Au@DHLA$_{56}$, (c) Au@DHLA$_{140}$, and (d) Au@DHLA$_{222}$ NPs. All scale bars = 20 nm.

The average diameters extracted from the TEM images (n > 200) are listed in Table 1. Higher inhomogeneities in nanoparticles shape and size dispersion can be observed for Au@DHLA$_{28}$ NPs dispersions (Figure 6) than for Au@DHLA$_{56}$, Au@DHLA$_{140}$, and Au@DHLA$_{222}$ NPs, respectively, which confirmed the results observed by UV−vis absorption. For that small ligand coverage, TEM studies indicate that the interparticle distance is reduced and that NPs start to coalesce and aggregate, with the extent of aggregation increasing as a function of storage time (vide infra). Moreover, we also noticed that solutions of Au@DHLA$_{28}$ NPs turned to a dark-gray color after a few days of storage, indicating particle irreversible aggregation.[53]

Hydrodynamic diameters of citrate-stabilized and DHLA-functionalized Au NPs were measured one day after the ligand exchange (Table 1). All Au NPs exhibit appropriate D_h values, which were larger than the metallic core (because of the drying process before TEM observations and solvatation layers in aqueous medium). The derived DLS size distributions (data not shown) were found to be monomodal with a relatively narrow distribution, confirming the absence of aggregation after the capping exchange and subsequent purification step of all Au NPs. However, hydrodynamic diameters measured for Au@DHLA NPs were determined not to be uniform and to be strongly dependent on the [DHLA]/[Au] ratio used for the ligand exchange. Au@DHLA$_{28}$ NPs exhibit a value of $D_h \approx 15$ nm, which is ∼2.3 times larger than the native citrate-stabilized Au NPs (6.5 nm). A strong decrease of D_h was observed when the [DHLA]/[Au] ratio increased. Au@DHLA$_{56}$, Au@DHLA$_{140}$ and Au@DHLA$_{222}$ NPs have D_h values close to that of the starting citrate-stabilized Au NPs, indicating that the ligand exchange was homogeneous onto these Au NPs and the lack of Au NPs coalescence during the capping exchange reaction.

The electric potential, referred to as zeta potential (ζ), which controls the colloidal stability and interparticle interactions, was also determined for the 5 sets of Au NPs (Table 1). ζ values obtained confirmed the presence of negative charges on the surfaces of the Au NPs, due to the carboxylate groups of the citrate or DHLA ligands. After dialysis and at pH 7.4, citrate-stabilized Au NPs have a high negative charge of −51 mV. At the same pH value, the ζ potential values measured for Au@DHLA$_{28}$, Au@DHLA$_{56}$, Au@DHLA$_{140}$, and Au@DHLA$_{222}$ NPs are −44, −56, −66, and −63 mV, respectively. These values also confirmed the increase of capping density by the DHLA ligand when increasing the [DHLA]/[Au] ratio during the ligand exchange reaction.

Colloidal Stability of Au@DHLA NPs. Two types of experiments were conducted in order to assess the colloidal stability of Au@DHLA NPs either in their final medium of synthesis (i.e., PBS) or in the presence of a factor able to trigger aggregation such as salt (NaCl) and another dithiol (dithiothreitol).

First, for Au NPs coated by a layer of thioacid like DHLA, strong electrostatic forces should prevent the particles from contacting and aggregation above pH 4.8. However, these electrostatic forces are sensitive to salts present in the medium, which can cause bridging between NPs, thus leading to aggregation. Evaluation of the stability of Au@DHLA NPs in an electrolytic environment like PBS (pH 7.4, ionic strength = 150 mM) should not only provide information on how Au NPs potentially behave in biological media, but also allow to assess the ligand binding affinity to the nanocrystals.

DLS and UV−vis spectroscopy were first used to monitor the stability of Au NPs over a period of 50 days in PBS at 4 °C (Figure 7). Starting citrate-stabilized Au NPs were found to be highly sensitive to saline media and precipitated completely in 24 h when added to PBS. The density of the capping layer was found to have marked effects on the stability of Au@DHLA NPs in PBS. The measured D_h of Au@DHLA$_{28}$ NPs was found to increase with storage time in PBS and reached ∼150 nm after 50 days, indicating a clear aggregation of the native material (Figure 7a). This result is supported by the red-shift of the SPR band to 547 nm (Figure 7b) and confirms TEM data recorded for these NPs just after the purification step. Moreover, dispersions of these NPs became progressively

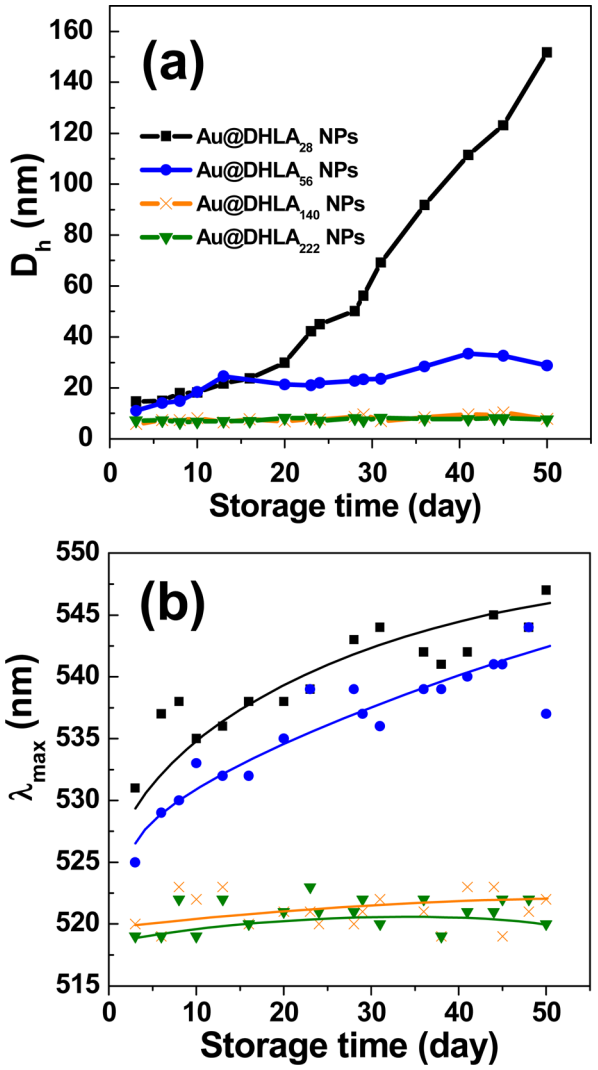

Figure 7. Stability studies of the different Au NPs ((■) Au@DHLA$_{28}$, (●) Au@DHLA$_{56}$, (×) Au@DHLA$_{140}$, (▼) Au@DHLA$_{222}$) stored at 4 °C in PBS versus storage time: evolution of (a) hydrodynamic diameters (D_h) and (b) surface plasmon resonance band maxima (λ_{max}).

unstable with time and changed color to dark-purple. Irreversible macroscopic precipitation was also observed after few days of storage at 4 °C.

The degree of aggregation was also found to be marked for Au@DHLA$_{56}$ NPs. Although a marked red shift from 522 nm at day 0 to more than 540 nm at day 45 was observed by UV−vis spectroscopy (Figure 7b), the increase of D_h is significantly less pronounced than that observed for Au@DHLA$_{28}$ NPs (D_h ≈ 30 nm after 50 days of storage) (Figure 7a). Neither a bathochromic shift of the SPR band maximum nor an increase of the D_h value were observed for Au@DHLA$_{140}$ and Au@DHLA$_{222}$ NPs, which were essentially unaffected in a PBS medium over 50 days of storage and exhibit the best colloidal stability.

Second, we explored the effects of adding an excess of NaCl on the colloidal stability of Au@DHLA NPs prepared using the various [DHLA]/[Au] ratios described above. Figures 8a and 8b show the evolution of D_h and of the SPR band, respectively, upon addition of Au@DHLA NPs in a 1 M NaCl solution (citrate-stabilized Au NPs were used as control samples).

The citrate-stabilized Au NPs changed color from red to violet immediately upon mixing with the salt solution and precipitated within 30 min. Au@DHLA$_{28}$ and Au@DHLA$_{56}$ NPs became progressively unstable with time (Figure 8a), and a strong agglomeration was already observed after 1 h (D_h = 1200 nm). In comparison, dispersions of Au@DHLA$_{140}$ and Au@DHLA$_{222}$ were found to be much more stable when dispersed in a 1 M NaCl solution with no aggregates formation. As shown in Figure 8b, the addition of 1 M NaCl caused a gradual shift of Au@DHLA$_{28}$ and Au@DHLA$_{56}$ NPs SPR band from 530 nm to 600 nm over 100 min, indicative of an unstability of these samples. The bathochromic shifts of the SPR band maxima were found to be less pronounced (from 532 nm to 583 nm and 547 nm for Au@DHLA$_{140}$ and Au@DHLA$_{222}$ NPs, respectively) and Au@DHLA$_{222}$ NPs remained dispersed and aggregate-free in 1 M NaCl solution at least for 24 h.

At last, we evaluated the formation of Au NPs aggregates in the presence of a 0.1 M 1,4-dimercapto-2,3-butanediol (also called dithiothreitol, DTT) solution. Since DTT has a great affinity for Au NPs, DHLA displacement by DTT should alter the photophysical properties of the Au NPs, including a red shift and a decrease of the SPR band and a change in the NPs dispersion color.[54−57] For citrate-stabilized Au NPs, a rapid D_h increase and a red shift of the SPR band maximum (from 522 nm to 570 nm in 10 min) were observed (see Figures 8c and 8d). A λ_{max} value of 595 nm was attained after 100 min, which suggests the formation of aggregates. Under the same experimental conditions, no color change and no sign of aggregation were observed for all Au@DHLA NPs, indicating a higher colloidal stability. More interestingly, a gradual shift of the SPR band maximum was observed for all NPs from ca. 530 nm to 525 nm after treatment with DTT (Figure 8d). It is likely that this blue shift is related to a surface-etching[47−51] of Au@DHLA NPs in the presence of the excess DTT. XPS was used to monitor the interaction of DTT with Au@DHLA$_{222}$ NPs. We chose these NPs, because they should be less sensitive to displacement by DTT, because of the high surface coverage in DHLA. As can be seen in Figure 9a, the Au 4f signal is only weakly affected by DTT. The Au 4f$_{7/2}$ binding energy is 83.66 eV after interaction with DTT, while it was 83.70 eV in the native Au@DHLA$_{222}$ NPs. Figure 9b shows two contributions for S 2p$_{3/2}$ (161.73 and 163.16 eV) and for S 2p$_{1/2}$ (162.89 and 164.32 eV) while only one signal was observed for S 2p$_{3/2}$ and for S 2p$_{1/2}$ in the starting NPs at 163.21 and 164.37 eV, respectively. These results indicate that the organic shell surrounding the Au core is composed of DHLA and DTT and that DTT, even used at high concentration (0.1 M), is unable to displace DHLA molecules from Au NPs surface. This may be related to similar affinities for Au NPs surface of DHLA and DTT. Au@DHLA NPs can probably accommodate the DTT ligand, which further behaves as a protective agent of the Au core.

Results obtained after these three stability tests demonstrate first that, because of its two anchoring groups to the Au metallic surface, DHLA provides enhanced stability to Au NPs in an aqueous solution, compared to single-thiol ligand-capped Au NPs, which are far less stable in electrolytic environments.[16,55−57] Second, the surface packing density of DHLA is a crucial parameter to enhance the stability of Au@DHLA NPs in aqueous solution, a high surface coverage affording NPs with the best colloidal stability.

Surface Packing Density of DHLA Controls NPs Reactivity with a Free Radical and Bovine Serum

dx.doi.org/10.1021/am3012752 | ACS Appl. Mater. Interfaces 2012, 4, 5790−5799

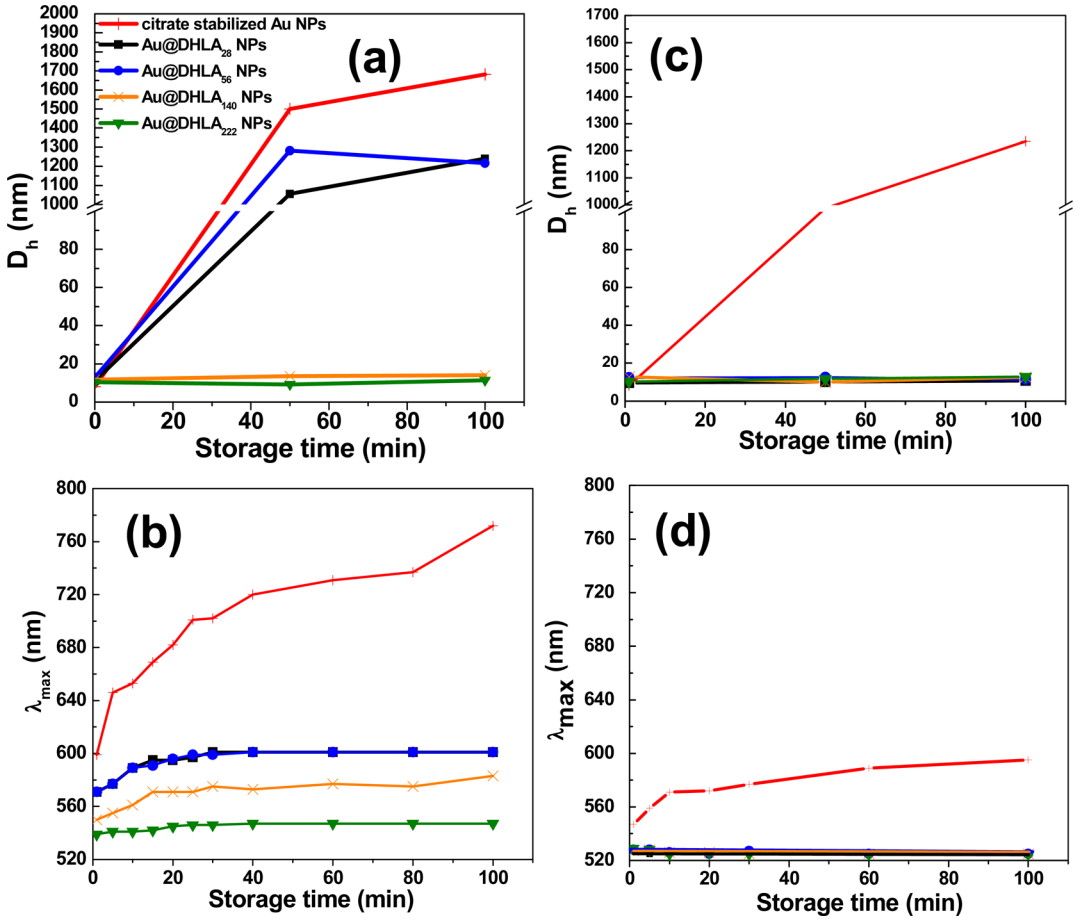

Figure 8. (a, c) Time-dependent hydrodynamic diameters and (b, d) λ_{max} evolution upon addition of citrate-stabilized Au NPs (+) and Au@DHLA NPs ((■) Au@DHLA$_{28}$, (●) Au@DHLA$_{56}$, (×) Au@DHLA$_{140}$, and (▼) Au@DHLA$_{222}$) in a 1 M NaCl solution (panels (a) and (b)) and in a 0.1 M DTT solution (panels (c) and (d)).

Albumin. Understanding the reactivity between molecules of biological relevance and Au NPs is crucial to predict the Au NPs fate in human body. Because of the rising interest of Au NPs for biomedical applications, research is investigating the detailed interactions between Au NPs and some molecules. Two types of molecules were presently tested: a free radical, 2,2′-azino-di(3-ethylbenzothiazoline-6-sulfonate, ABTS) to check the residual catalytic activity of Au NPs, and a protein of biological relevance, bovine serum albumin (BSA). The influence of the surface packing density on the behavior of Au@DHLA NPs toward the molecules was evaluated. In all of these assays, Au@DHLA$_{28}$ NPs were not tested due to their low stability highlighted in the previous paragraph.

Previous works have already reported that gold and other noble-metal NPs can react with free radicals, for example 1,1-diphenyl-2-picrylhydrazyl (DPPH$^{\bullet}$).[58−60] Nevertheless, the reaction with this radical is usually followed at a wavelength of 515 nm, which overlaps with the SPR band maxima. Therefore, novel methods were devoted to limit this phenomenon via HPLC analysis, for instance.[60] In this study, Au NPs catalyze a hydrogen atom transfer to the probe. Although the DPPH$^{\bullet}$ reaction requires an organic medium, the ABTS$^{\bullet+}$ radical, which also is widely used to evaluate the radical scavenging properties of antioxidants, can react in aqueous solution, which mimics the physiological environment more accurately. Therefore, this in situ-generated radical was chosen to evaluate the residual Au NPs metallic core catalytic activity. In this study, the surface capping density of Au NPs is hypothesized to minimize the interaction of free radicals with the surface of Au NPs.[19] To support this hypothesis, Au NPs at different concentrations (10−90 nM) were reacted in a ABTS$^{\bullet+}$ solution. As shown in Figure 10a, the initial concentration of ABTS$^{\bullet+}$ gradually decreased when Au NPs concentration increased for all types of particles.

The half-maximum values (EC50) of the concentration−response curves were calculated and the results were as follows: 11 ± 1, 19 ± 1, 24 ± 1, 26 ± 1 nM for citrate-stabilized Au NPs, Au@DHLA$_{56}$, Au@DHLA$_{140}$, and Au@DHLA$_{222}$ NPs, respectively. The obtained values of citrate-stabilized Au NPs, Au@DHLA$_{56}$ were significantly different of what was calculated for Au@DHLA$_{140}$ and Au@DHLA$_{222}$ ($p < 0.05$). Moreover, no statistically difference was highlighted between the two last cited Au NPs. Therefore, DHLA capping seems to bring a better inertia toward highly reactive molecules. Moreover, the surface capping density is a key to controlling the reaction between Au NPs and free radicals.

The interaction of particles with albumin is usually the first step to predict the object becoming in bloodstream since it is quantitatively the most important circulating protein (38 to 48 g/L) with a fundamental role into oncotic pressure, transport of molecules, and antioxidant property.[61] In this work, we evaluated how the surface packing density of Au NPs influences the reactivity toward bovine serum albumin (BSA), which possesses 76% homology, compared to the human protein.[62]

dx.doi.org/10.1021/am3012752 | ACS Appl. Mater. Interfaces 2012, 4, 5790−5799

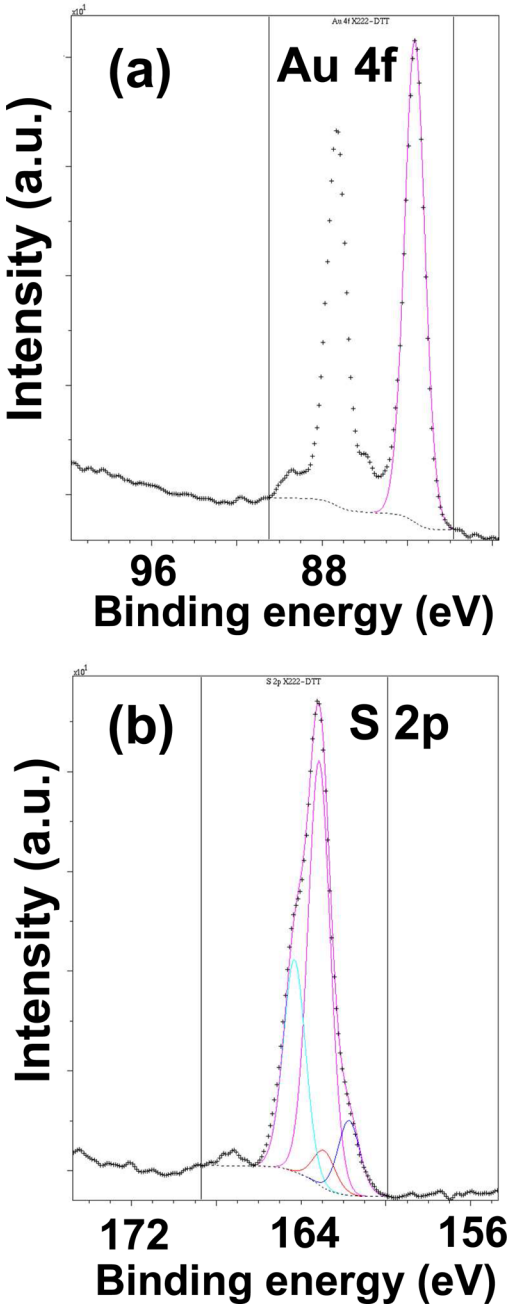

Figure 9. XPS spectra of Au@DHLA$_{222}$ NPs after interaction with DTT: (a) Au 4f region and (b) S 2p region.

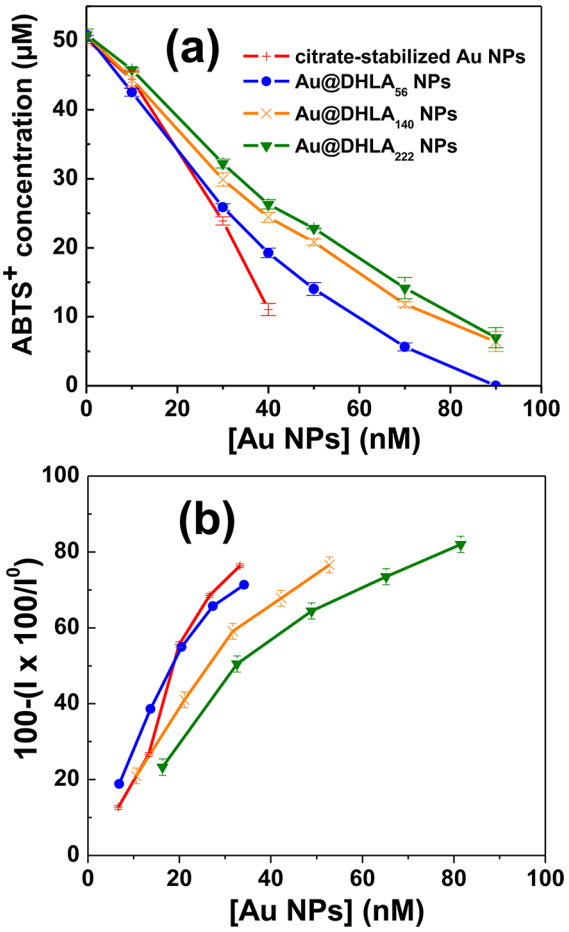

Figure 10. Reactivity between (+) Au NPs (citrate-stabilized Au NPs and Au@DHLA NPs: (●) Au@DHLA$_{56}$, (×) Au@DHLA$_{140}$, Au@DHLA$_{222}$ (▼)) and (a) 2,2′-azino-bis(3-ethylbenzothiazoline-6-sulfonic acid) radical ABTS$^{\bullet+}$ and (b) bovine serum albumin (BSA). Fluorescence intensities of the protein were recorded in the absence (I°) and the presence (I) of Au NPs.

BSA fluorescence quenching, as a function of Au NPs concentration, was studied (Figure 10b). The results showed that, regardless of the surface capping density, all Au NPs interact with BSA. Nevertheless, the Stern−Volmer constants were calculated as follows: 0.091 ± 0.003, 0.068 ± 0.002, 0.056 ± 0.003 and 0.047 ± 0.003 nM^{-1} for citrate-stabilized Au NPs, Au@DHLA$_{56}$, Au@DHLA$_{140}$ and Au@DHLA$_{222}$ NPs, respectively. Stern−Volmer constant obtained in the case of the densest surface packing (Au@DHLA$_{222}$) was significantly different ($p < 0.001$), compared to all of the other cappings. It is well-known that the quenching between BSA and Au NPs occurs via an interaction with tryptophan located at position 212, in a hydrophobic domain, which changes its fluorescence after modification of its molecular environment.[62] Currently, two mechanisms are highlighted to understand how Au NPs can bind BSA and as a consequence, quenches the amino acid fluorescence:[63] First, the electrostatic binding, which is based on the fact that even though BSA is globally negatively charged at physiological pH, 60 positively charged lysine residues are located on the protein surface able to interact with oppositely charged groups through electrostatic interactions. Second, the displacement mechanism, in which Au NPs capping ligand is displaced after adsorption of BSA onto the gold core.

With regard to citrate-stabilized Au NPs, the interaction occurs mainly through the first mechanism, but the second one is not excluded.[63] If DHLA capping is now considered, capping ligand displacement may not occur because of the presence of two S atoms that covalently bind the Au NPs core. Therefore, this gives superiority to DHLA over citrate as a capping ligand, especially if the packing density of Au@DHLA$_{222}$ is taken into consideration. Moreover, even if Au@DHLA NPs bind BSA, the most important capping was able to limit this interaction, to some extent. These experimentations are very important with regard to testing these NP platforms as future drug delivery systems, since it is now well-described that protein binding on nano objects induces fast internalization by cells through multiple receptor uptake.[64] Indeed, this phenomenon helps antigen-presenting cells recognition, (macrophages, B cells, and dendritic cells, which are efficient in nonself internalization),

dx.doi.org/10.1021/am3012752 | ACS Appl. Mater. Interfaces 2012, 4, 5790−5799

and, finally, induces fast clearance from bloodstream.[65] Therefore, protein binding on NPs surface will directly influence the pharmacokinetic behavior of a nano object (half-life and distribution to the targeted site, for instance). But, thanks to the presence of the carboxylic acid groups of DHLA on Au NPs surface, these particles offer the possibility to be further functionalized by the grafting of a drug of therapeutic relevance and also poly(ethylene glycol). Indeed, this polymer is usually used to create a steric barrier to avoid protein adsorption on NPs in order to improve the object half-life in bloodstream.[65] As a consequence, Au@DHLA$_{222}$ NPs will be chosen and chemically modified to finally investigate the impact on macrophage physiology of this platform, offering both, a pharmaceutical application and stealthiness toward the antigen-presenting cells.

4. CONCLUSIONS

Citrate-capped gold nanoparticles (Au NPs) with an average diameter of ca. 5 nm were coated with dihydrolipoic acid (DHLA), using a cap-exchange method. The influence of the molar ratio of DHLA to Au on the properties and on the stability of Au@DHLA NPs produced was investigated. Among the four sets of Au NPs prepared (Au@DHLA$_{28}$, Au@DHLA$_{56}$, Au@DHLA$_{140}$, and Au@DHLA$_{222}$), Au@DHLA NPs with the highest ligand surface density exhibit the best colloidal stability under in vitro physiological conditions. The superior stability of Au@DHLA$_{140}$ and Au@DHLA$_{222}$ NPs in saline medium results from the combined effects of (i) the tight binding offered by the bidentate dithiol group of DHLA on Au NPs surfaces, and (ii) the more homogeneous surface coverage of Au NPs provided by high [DHLA]/[Au] ratios. Finally, Au@DHLA$_{222}$ showed the best inertia toward a free radical and albumin, thus it becomes an ideal candidate for further biomedical application.

AUTHOR INFORMATION

Corresponding Author

*Tel.: +33 3 83 17 50 53. E-mail: raphael.schneider@univ-lorraine.fr.

Notes

Notes. The authors declare no competing financial interest.

ACKNOWLEDGMENTS

Authors gratefully acknowledge Dr. Lavinia Balan (IS2M, LRC 7228, Université de Haute Alsace, Mulhouse, France) for TEM measurements and Debora Gościk (Poznan University of Medical Sciences, Poznan, Poland) for technical assistance during stability studies.

REFERENCES

(1) De, M.; Ghosh, P. S.; Rotello, V. M. *Adv. Mater.* **2008**, *20*, 4225−4241.
(2) Rosi, N. L.; Mirkin, C. A. *Chem. Rev.* **2005**, *105*, 1547−1562.
(3) Alivisatos, P. *Nat. Biotechnol.* **2004**, *22*, 47−52.
(4) Haes, A. J.; Hall, W. P.; Chang, L.; Klein, W. L.; Van Duyne, R. P. *Nano Lett.* **2004**, *4*, 1029−1034.
(5) Boisselier, E.; Astruc, D. *Chem. Soc. Rev.* **2009**, *38*, 1759−1782.
(6) Warsi, M. F.; Adams, R. W.; Duckett, S. B.; Chechik, V. *Chem. Commun.* **2010**, *46*, 451−453.
(7) Gupta, A. K.; Gupta, M. *Biomaterials* **2005**, *26*, 3995−4021.
(8) Joshi, P.; Chakraborty, S.; Dey, S.; Shanker, V.; Ansari, Z. A.; Singh, S. P.; Chakrabarti, P. *J. Colloid Interface Sci.* **2011**, *355*, 402−409.
(9) Paciotti, G. F.; Kingston, D. G. I.; Tamarkin, L. *Drug. Dev. Res.* **2006**, *67*, 47−54.
(10) Srisombat, L.; Jamison, A. C.; Lee, T. R. *Colloids Surf. A: Physicochem. Engineer. Aspects* **2011**, *390*, 1−19.
(11) Rao, C. N. R.; Mèuller, A.; Cheetham, A. K., *The chemistry of nanomaterials: synthesis, properties and applications in 2 volumes.* Weinheim: Wiley-VCH: Allemagne, 2004.
(12) Templeton, A. C.; Wuelfing, W. P.; Murray, R. W. *Acc. Chem. Res.* **2000**, *33*, 27−36.
(13) Turkevich, J.; Stevenson, P. C.; Hillier, J. *Discuss. Faraday Soc.* **1951**, *11*, 55−75.
(14) Kimling, J.; Maier, M.; Okenve, B.; Kotaidis, V.; Ballot, H.; Plech, A. *J. Phys. Chem. B* **2006**, *110*, 15700−15707.
(15) Brown, K. R.; Walter, D. G.; Natan, M. J. *Chem. Mater.* **2000**, *12*, 306−313.
(16) Brust, M.; Walker, M.; Bethell, D.; Schiffrin, D. J.; Whyman, R. *J. Chem. Soc., Chem. Comm.* **1994**, 801−802.
(17) Jans, H.; Stakenborg, T.; Jans, K.; de Broek, B. V.; Peeters, S.; Bonroy, K.; Lagae, L.; Borghs, G.; Maes, G. *Nanotechnology* **2010**, *21*, 285608.
(18) Roux, S.; Garcia, B.; Bridot, J. -L.; Salomé, M.; Marquette, C.; Lemelle, L.; Gillet, P.; Blum, L.; Perriat, P.; Tillement, O. *Langmuir* **2005**, *21*, 2526−2536.
(19) Biswas, M.; Dinda, E.; Rashid, M. H.; Mandal, T. K. *J. Colloid Interface Sci.* **2012**, *368*, 77−85.
(20) Mattoussi, H.; Mauro, J. M.; Goldman, E. R.; Anderson, G. P.; Sundar, V. C.; Mikulec, F. V.; Bawendi, M. G. *J. Am. Chem. Soc.* **2000**, *122*, 12142−12150.
(21) Stewart, M. H.; Susumu, K.; Mei, B. C.; Medintz, I. L.; Delehanty, J. B.; Blanco-Canosa, J. B.; Dawson, P. E.; Mattoussi, H. *J. Am. Chem. Soc.* **2010**, *132*, 9804−9813.
(22) Aldeek, F.; Mustin, C.; Balan, L.; Roques-Carmes, T.; Fontaine-Aupart, M. P.; Schneider, R. *Biomaterials* **2011**, *32*, 5459−5470.
(23) Kim, T.; Lee, C. H.; Joo, S. W.; Lee, K. *J. Colloid Interface Sci.* **2008**, *318*, 238−243.
(24) Kim, T.; Lee, K.; Gong, M. S.; Joo, S. W. *Langmuir* **2005**, *21*, 9524−9528.
(25) Balasubramanian, S. K.; Yang, L.; Yung, L. -Y. L.; Ong, C. -N.; Ong, W. -Y.; Yu, L. E. *Biomaterials* **2010**, *31*, 9023−9030.
(26) Chompoosor, A.; Han, G.; Rotello, V. M. *Bioconjugate Chem.* **2008**, *19*, 1342−1345.
(27) Zhang, F.; Skoda, M. W. A.; Jacobs, R. M. J.; Zorn, S.; Martin, R. A.; Martin, C. M.; Clark, G. F.; Goerigk, G.; Schreiber, F. *J. Phys. Chem. A* **2007**, *111*, 12229−12237.
(28) Zhu, T.; Vasilev, K.; Kreiter, M.; Mittler, S.; Knoll, W. *Langmuir* **2003**, *19*, 9518−9525.
(29) Gofberg, I.; Mandler, D. *J. Nanopart. Res.* **2010**, *12*, 1807−1811.
(30) Bogliotti, N.; Oberleitner, B.; Di-Cicco, A.; Schmidt, F.; Florent, J. C.; Semetey, V. J. *Colloid Interf. Sci.* **2011**, *357*, 75−81.
(31) Zhang, G.; Yang, Z.; Lu, W.; Zhang, R.; Huang, Q.; Tian, M.; Li, L.; Liang, D.; Li, C. *Biomaterials* **2009**, *30*, 1928−1936.
(32) Li, Z.; Jin, R.; Mirkin, C. A.; Letsinger, R. L. *Nucleic Acids Res.* **2002**, *30*, 1558−1562.
(33) Zhang, S.; Leem, G.; Srisombat, L. −o.; Lee, T. R. *J. Am. Chem. Soc.* **2008**, *130*, 113−120.
(34) Srisombat, L. −o.; Park, J. −S.; Zhang, S.; Lee, T. R. *Langmuir* **2008**, *24*, 7750−7754.
(35) Tang, Z.; Xu, B.; Wu, B.; Robinson, D. A.; Bokossa, N.; Wang, G. *Langmuir* **2011**, *27*, 2989−2996.
(36) Tang, Z.; Ahuja, T.; Wang, S.; Wang, G. *Nanoscale* **2012**, *4*, 4119−4124.
(37) Moini, H.; Packer, L.; Saris, N. E. L. *Toxicol. Appl. Pharmacol.* **2002**, *182*, 84−90.
(38) Leroy, P.; Sapin-Minet, A.; Pitarch, A.; Boudier, A.; Tournebize, J.; Schneider, R. *Nitric Oxide-Biol. Chem.* **2011**, *25*, 54−56.
(39) Tournebize, J.; Sapin-Minet, A.; Schneider, R.; Boudier, A.; Maincent, P.; Leroy, P. *Talanta* **2011**, *83*, 1780−1783.
(40) Lewis, D. J.; Day, T. M.; MacPherson, J. V.; Pikramenou, Z. *Chem. Commun.* **2006**, *13*, 1433−1435.

(41) Re, R.; Pellegrini, N.; Proteggente, A.; Pannala, A.; Yang, M.; Rice-Evans, C. *Free Radic. Biol. Med.* **1999**, *26*, 1231−1237.
(42) Pramanik, S.; Banerjee, P.; Sarkar, A.; Bhattacharya, S. C. *J. Lumin.* **2008**, *128*, 1969−1974.
(43) Möller, M.; Denicola, A. *Biochem. Mol. Biol. Educ.* **2002**, *30*, 175−178.
(44) Whetten, R. L.; Khowy, J. T.; Alvarez, M. M.; Murthy, S.; Vezmar, I.; Wang, Z. L.; Stephens, P. W.; Cleveland, C. L.; Luedtke, W. D.; Landman, U. *Adv. Mater.* **1996**, *8*, 428−433.
(45) Lin, S. −Y.; Tsai, Y. −T.; Chen, C. −C.; Lin, C. −M.; Chen, C. −h. *J. Phys. Chem. B* **2004**, *108*, 2134−2139.
(46) Vargas, M. C.; Giannozzi, P.; Selloni, A.; Scoles, G. *J. Phys. Chem. B* **2001**, *105*, 9509−9513.
(47) Schaaff, T. G.; Whetten, R. L. *J. Phys. Chem. B* **1999**, *103*, 9394−9396.
(48) Tsunoyama, H.; Nickut, P.; Negishi, Y.; Al-Shamery, K.; Matsumoto, Y.; Tsukuda, T. *J. Phys. Chem. C* **2007**, *111*, 4153−4158.
(49) Qian, H.; Zhu, M.; Lanni, E.; Zhu, Y.; Bier, M. E.; Jin, R. *J. Phys. Chem. Lett.* **2009**, *113*, 17599−17603.
(50) Muhammed, M. A. M.; Verma, P. K.; Pal, S. K.; Retnakumari, A.; Koyakutty, M.; Nair, S.; Pradeep, T. *Chem.—Eur. J.* **2010**, *16*, 10103−10112.
(51) Pettibone, J. M.; Hudgens, J. W. *ACS Nano* **2011**, *5*, 2989−3002.
(52) Vance, A. L.; Willey, T. M.; Nelson, A. J.; van Buuren, T.; Bostedt, C.; Terminello, L. J.; Fox, G. A.; Engelhard, M.; Baer, D. *Langmuir* **2002**, *18*, 8123−8128.
(53) Link, S.; El-Sayed, M. A. *J. Phys. Chem. B* **1999**, *103*, 4212−4217.
(54) Mei, B. C.; Oh, E.; Susumu, K.; Farrell, D.; Mountziaris, T. J.; Mattoussi, H. *Langmuir* **2009**, *25*, 10604−10611.
(55) Oh, E.; Susumu, K.; Goswami, R.; Mattoussi, H. *Langmuir* **2010**, *26*, 7604−7613.
(56) Qiao, F. Y.; Liu, J.; Li, F. R.; Kong, X. L.; Zhang, H. L.; Zhou, H. X. *Appl. Surf. Sci.* **2008**, *254*, 2941−2946.
(57) Kim, J. -Y.; Lee, J. -S. *Nano Lett.* **2009**, *9*, 4564−4569.
(58) Isono, R.; Yoshimura, T.; Esumi, K. *J. Colloid Interface Sci.* **2005**, *288*, 177−83.
(59) Nie, Z.; Liu, K. J.; Zhong, C. J.; Wang, L. F.; Yang, Y.; Tian, Q.; Liu, Y. *Free Radic. Biol. Med.* **2007**, *43*, 1243−54.
(60) Boudier, A.; Tournebize, J.; Bartosz, G.; El Hani, S.; Bengueddour, R.; Sapin-Minet, A.; Leroy, P. *Anal. Chim. Acta* **2012**, *711*, 97−106.
(61) Candiano, G.; Petretto, A.; Bruschi, M.; Santucci, L.; Dimuccio, V.; Prunotto, M.; Gusmano, R.; Urbani, A.; Ghiggeri, G. M. *J. Proteomics* **2009**, *73*, 188−195.
(62) Chakraborty, S.; Joshi, P.; Shanker, V.; Ansari, Z. A.; Singh, S. P.; Chakrabarti, P. *Langmuir* **2011**, *27*, 7722−7731.
(63) Brewer, S. H.; Glomm, W. R.; Johnson, M. C.; Knag, M. K.; Franzen, S. *Langmuir* **2005**, *21*, 9303−9307.
(64) Chithrani, B. D.; Ghazani, A. A.; Chan, W. C. W. *Nano Lett.* **2006**, *6*, 662−668.
(65) Owens, D. E., III; Peppas, N. A. *Int. J. Pharmaceut.* **2006**, *307*, 93−102.